## Emergent chirality in a polar meron to skyrmion transition revealed by 4D-STEM

Yu-Tsun Shao<sup>1</sup>, Sujit Das<sup>2</sup>, Zijian Hong<sup>3</sup>, Ruijuan Xu<sup>4</sup>, Swathi Chandrika<sup>5</sup>, Fernando Gómez-Ortiz<sup>6</sup>, Pablo García-Fernández<sup>6</sup>, Long-Qing Chen<sup>7</sup>, Harold Hwang<sup>4</sup>, Javier Junquera<sup>6</sup>, Lane Martin<sup>2</sup>, Ramamoorthy Ramesh<sup>8</sup> and David Muller<sup>9</sup>

<sup>1</sup>School of Applied and Engineering Physics, Cornell University, Ithaca, NY, USA, Ithac, New York, United States, <sup>2</sup>University of California, Berkeley, United States, <sup>3</sup>Zhejiang University, United States, <sup>4</sup>Stanford University, United States, <sup>5</sup>Cornell University, United States, <sup>6</sup>Universidad de Cantabria, United States, <sup>7</sup>Penn State University, United States, <sup>8</sup>University of California, Berkeley, Berkeley, California, United States, <sup>9</sup>School of Applied and Engineering Physics, Cornell University, Ithaca, NY, USA, Ithaca, New York, United States

Topological structures in ferroic can produce particle-like objects such as skyrmions and merons, with real-space swirling arrangements of the order parameter that not only have mathematical beauty but hold promise for potential applications in next generation nanodevices such as racetrack memories [1]. Although the focus has largely been on spin textures in magnets, in recent years analogous electric dipolar textures have been realized in multiple systems including ferroelectric heterostructures of (PbTiO<sub>3</sub>)<sub>n</sub>/(SrTiO<sub>3</sub>)<sub>n</sub> [2]. Fundamentally different from their magnetic counterparts, polar vortices and skyrmions exhibit new functionalities such as emergent chiral order and negative capacitance [3-5]. As the polar textures are intrinsically nm-scale and dynamic, developing methods for visualizing and characterizing their detailed 3D structure is a critical step in understanding their properties and exploring possible phase transitions.

Given the strong electrostrictive coupling between polarization and strain, artefacts are inevitable in characterizing ferroelectric crystals using conventional scanning transmission electron microscopy (STEM) imaging modes such as high-angle annular dark field (HAADF) or differential phase contrast (DPC), with which local electric field or atomic displacements were typically measured. Since all perovskite ferroelectrics are ferroelastic by nature [6], the crystal mis-tilt is ubiquitous and intrinsically inevitable across domain boundaries and in complex topological structures. A slight crystal mis-tilt of as small as 0.1° may complicate and dominate the interpretation of DPC-/HAADF-STEM images [7,8]. To decouple the polarization information from crystal mis-tilt artifacts, we developed a new 4D-STEM technique by recording polarity-sensitive Kikuchi bands and chirality-sensitive Bijvoet pairs at every probe position using an electron microscopy pixel array detector (EMPAD) [9]. Using this approach, figure 1 shows detailed chiral dipolar textures and their 3D chirality in free-standing ferroelectric membranes despite buckling that would foil the simpler methods [10].

We next show that by manipulating the temperature and elastic boundary conditions, the polar skyrmions (topological charge of +1) were deformed and transformed into pairs of polar merons, that have a different topology as characterized by a topological charge of +1/2 [11]. This topological phase transition is driven by strain, as evidenced by the in-plane lattice parameter anisotropy mapped with exit wave power cepstrum (EWPC) analysis from the same 4D-STEM datasets [12], Figure 2.

The results of this presentation show how 4D-STEM in combination with a fast, high dynamic range EMPAD detector provides a new platform for the robust imaging of polarization, chirality, and strain of complex topological textures such as skyrmions and merons in oxide heterostructures [13].

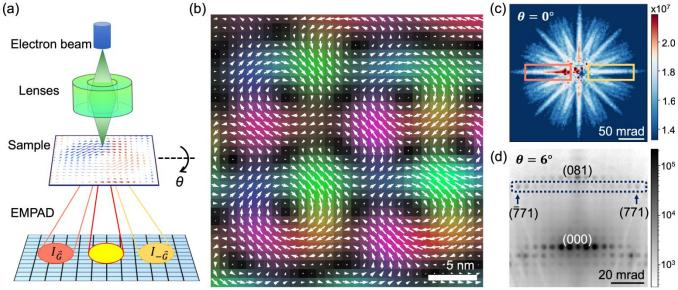


**Figure 1.** Figure 1. Imaging polarity and chirality for a ferroelectric meron lattice via 4D-STEM. (a). Schematic of 4D-STEM with a tilted sample and an EMPAD; (b). Polarization of Bloch-type meron lattice in the [(PbTiO3)16/(SrTiO3)16]8 heterostructure measured at 373 K. (c) & (d). Representative CBED patterns acquired with sample tilts at (c) 0° and (d) 6° away from the [001] zone axis. The polarity-sensitive Kikuchi bands (boxes in (c)) give a robust measure of polarization, independent of tilt. The Bijvoet pairs in the HOLZ (arrows in (d)) provide the 3D polar information needed to determine chirality.

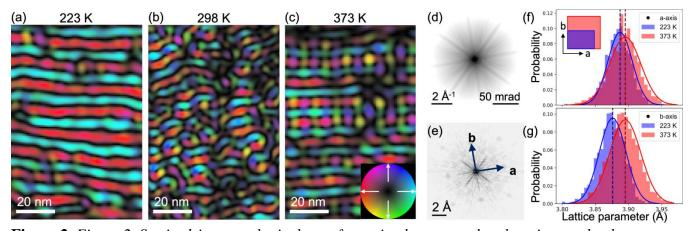


**Figure 2.** Figure 2. Strain-driven topological transformation between polar skyrmions and polar merons. (a-c). In-plane polarization maps of dipolar textures reconstructed from 4D-STEM datasets acquired at various temperatures. (d). Representative CBED pattern and its (e) EWPC transform showing real-space points corresponding to in-plane lattice parameters a & b. Histograms of lattice parameters along (f) a-and (g) b-axis, at temperatures of 223 K (blue) and 373 K (red). Inset in (f) is an exaggerated cartoon indicating the film is more rectangular at 223 K than at 373 K.

## References

- [1] N. Nagaosa and Y. Tokura, Nature Nanotechnology 8 (2013), 899.
- [2] S. Das, et al., Nature 568 (2019), 368.
- [3] A. K. Yadav et al., Nature 565 (2019), 468.
- [4] P. Shafer et al., PNAS 115 (2018), 915.
- [5] S. Das, et al., Nature Materials 20 (2020), 194.
- [6] K. Aizu, J. Phys. Soc. Jpn. 28 (1970), 706.
- [7] I. MacLaren et al., Ultramicroscopy 154 (2015), 57.
- [8] Y.-T. Shao et al., Microscopy and Microanalysis 25 (Suppl 2), 1938 (2019).
- [9] M. W. Tate et al., Microscopy and Microanalysis 22 (2016), 237-249.
- [10] D. Lu et al., Nature Materials 15 (2016), 1255.
- [11] Y.-T. Shao et al., arXiv:2101.04545 (2020).
- [12] E. Padgett et al., Ultramicroscopy 214 (2020), 112994.
- [13] Work supported by the AFOSR Hybrid Materials MURI, award # FA9550-18-1-0480. Facilities supported by the National Science Foundation (DMR-1429155, DMR-1539918, DMR-1719875)